International Journal of Mechanical Engineering and Technology (IJMET)
Volume 10, Issue 08, August 2019, pp. 61-77. Article ID: IJMET_10_08_005
Available online at http://www.iaeme.com/ijmet/issues.asp?JType=IJMET&VType=10&IType=8
ISSN Print: 0976-6340 and ISSN Online: 0976-6359

EXPERIMENTAL AND NUMERICAL INVESTIGATIONS ON HEAT TRANSFER AND FRICTION LOSS OF FUNCTIONALIZED GNP NANOFLUIDS

K.H. Solangi, S. Sharif, Ibrahim Ogu Sadiq and M.J. Hisam
School of Mechanical Engineering, Universiti Teknologi Malaysia, Johor Bahru 81310, Johor Malaysia.

ABSTRACT

Heat transfer and friction loss characteristics of functionalized graphene nanoplatelet-based water (GNP-water) nanofluids are analyzed numerically and experimentally. A horizontal copper test section of 4 mm in diameter was used to run the experiment in close conduit flow. In the numerical analysis for two-phase flow mixture model, the velocity of nanofluids and profile temperature were assumed and in total 50 simulation cases, 2 different heat fluxes, 4 concentrations at Re range of 3900–11,700 were investigated. In the results, significant enhancement was obtained in the thermal conductivity which increased up to 32%. After validation of the results, the highest enhancement in heat transfer coefficient and friction factor was obtained up to 119% and 10.2% by loading 0.1wt% of GNP-water nanofluids. It was perceived that heat transfer coefficient increases with increasing concentration of GNP-water nanofluids and flow Reynolds number (Re). The numerical and experimental results showed the good agreement with a maximum error of less than 4%. The experimental and numerical results reveal that the GNP-water can function as working fluids in heat transfer applications and can provide good alternatives to conventional working fluids in the thermal fluid systems.

Key words: Heat transfer, nanofluids, copper, turbulent flow, graphene nanoplatelet, propylene glycol.

Cite this Article K.H. Solangi, S. Sharif, Ibrahim Ogu Sadiq and M.J. Hisam, Experimental and Numerical Investigations on Heat Transfer and Friction Loss of Functionalized GNP Nanofluids, International Journal of Mechanical Engineering and Technology, 10(8), 2019, pp. 61-77.
http://www.iaeme.com/IJMET/issues.asp?JType=IJMET&VType=10&IType=8

1. INTRODUCTION

Currently, research on heat transfer augmentation is one of the most fascinating subjects for scientists working on the thermal engineering field. However, in this area fluid flow in

microchannels have becoming the hot topic. Though, microchannels are being used in several engineering disciplines due to their high heat removal density in a small space and volume [1-3]. Still, the enhanced thermal performance and improved thermo-physical properties of the working fluid engaging the researchers focus in optimizing the design of heat exchangers and use the nanosized particles in to the basefluid. As in many heat transfer applications, the conventional thermal fluids (ethylene glycol and water) are considered as coolants, while the thermal conductivity of those liquids are lower than those of most solids [4-7]. Therefore, to achieve the enhancement in heat transfer with limited temperature changes, the scientists have endeavored to add nanoparticles into liquid. However, the experimental and analytical research have proven that the nanofluids have higher thermal conductivity than the basefluids and it significantly can improve the enhancement in heat transfer [8-11]. Nanofluids have been attempted in several applications including solar thermal systems, refrigeration's systems, electronic cooling systems, automobiles, heat exchangers and medical applications etc [12-16]. There are various types are nanofluids being used such as metal oxide Al_2O_3, SiO_2, TiO_2, Fe_2O_3, CuO etc and non-metals CNT, GO and GNP etc [17-20]. However, carbon-based nanoparticles such as graphene nanoplatelet (GNP) has the higher thermal conductivity compared to the metal oxides. Therefore, it could produce the higher thermal performance. Baby and sundara [21] prepared the cobalt oxide decorated hydrogen exfoliated graphene (Co_3O_4-Graphene). However, they synthesized the Co_3O_4-Graphene by chemical reaction, and it was functionalized by acid treatment and was further decorated with silver. They achieved the 28% increment in thermal conductivity at 0.05% volume concentration. Along with the higher thermal conductivity they achieved highly stable nanofluids. Zhou et el [22] used the oscillating heat pipe to study the heat transfer performance by using graphene nanofluids. For the preparation of nanofluids they used the GNPs and distilled water and the volume concentrations from 1.22 to 16.8 % at heating power range of 10 -100W. however, at filling ratio of 55-70% the thermal resistances of the oscillating heat pipe (OHP) with GNP nanofluids were found lower compared to the basefluid, which could be proven that the adding GNPs to DW can improve the heat transfer performance. Ahmed et al [23] heat transfer coefficient and friction loss of multiwalled carbon nanotubes and graphene nanoplatelets (MWCNTs/GNPs) water based nanofluids. The weight concentration was used from 0.075-0.25wt%. They achieved 43% improvement in heat transfer coefficient at 0.25 wt% of MWCNTs/0.035wt% GNP at Re of 200. Also, they achieved the 11% rise in pressure drop. Similarly, Atiyeh et al [24] used the GNP and MWCNTs based diesel oil. They prepared the nanofluids by both techniques by covalent and no-covalent functionalization method. They observed that the covalent functionalized graphene has a higher heat transfer coefficient compared to non-covalent one. Also, they achieved the stable nanoflouids even after 30 days. Javier et al [25] used the functionalized GNP nanofluids by using the basefluid as water and propylene glycol mixtures. They investigated the rheological behavior of the nanofluids at wt% of 0.25 1 wt %. They confirmed the Newtonian behavior of all the sample by examining the viscosity curves in the shear rate range from 10 – 1000 s^{-1} and at temperature range of 283.15 – 353.15 k. Hooman et al [26] used the GNP/platinum hybrid nanofluid to examine the pressure drop and heat transfer performance of graphene based nanofluids. They prepared the nanofluids at wt % of 0.02 and 0.1% at Reynolds range of 5000 – 17500. However, they observed that the Nusselt number (Nu) elevation and enhancement in heat transfer coefficient are highly reliant on Re and the weight percentage of the nanofluids. However, they achieved the Nu which was 28.48%. Emad et el [27] studied the heat transfer performance of graphene based nanofluids and to solve the continuity, in the turbulent flow model they used the finite volume method (with standard k-Ɛ). Throughout in their numerical study the maximum error was found up to 5%. However, they obtained the enhancement in Nu which was up to 3-83% and the increment in pressure loss was achieved in the range of 0.4% to 14%. Sajjad et al [12] used the graphene oxide/ethylene glycol water based nanofluids to

numerically examine the convective heat transfer characteristics. In this experiment, single phase model approach was used to investigate the heat transfer coefficient and pressure loss. The weight percentage and Reynolds range were used up to 0.01-0.1 wt% and 40-2000 respectively. They achieved the improvement in heat transfer coefficient up to 13% at 0.1 wt%. Also, they observed that by increasing the Re and weight concentration the pressure drop also increased. However, only limited research has been done on the convective heat transfer of functionalized GNP nanofluids by using numerical and experimental investigations [28-31].

To predict the values and data validation the numerical investigation of heat transfer characteristics is essential which can be can be achieved by using single phase, two phase and multi-phase model approach. Mostly researchers have been approaching the single-phase and two-phase model. However, two-phase model gives the more accurate heat transfer numerical results compared to the other approaches [32-37]. The numerical and experimental approach requires an effective approach to understand the fundamental of heat transfer analysis, thermophysical properties and the use of potential nanofluids. Most of the numerical investigations specially in carbon based nanofluids have by tow phase model have not been validated with the experimental data. However, along with the experimental analysis, to numerically validate the experiment is very important. Several researchers have been studying individually on numerical and experimental analysis of heat transfer of metal oxide of carbon based nanofluids. However, there is no complete study has been found on the heat transfer performance of functionalized graphene nanoplatelets which could elaborate the nanoparticles morphology, basefluid, thermal performance in both numerically and experimentally.

In this study, a combined numerical and experimental methods were used to investigate the thermo-physical properties and heat transfer performance of propylene glycol related graphene nanoplatelets based water nanofluids (GNP-water). To achieve the highly dispersed nanofluids the nanofluids were developed by functionalization approach [38-41]. The pristine GNP and GNP-water nanofluids were characterized with different techniques such as TEM, SEM, FTIR, Raman etc. For numerical study of GNP-water nanofluids, the two-phase modeling approach was performed. It is a relatively simple approach for considering the higher weight percentage of nanoparticles. The effects of GNP-water nanofluids flowrate and inlet temperature are discussed as well. However, the main goal of this study is to examine the variation of convective heat transfer coefficient of GNP-water nanofluids and friction loss analysis. Further, to predict numerically the heat transfer performance of GNP-water nanofluids by assuming temperature and velocity parameters and to compare with the experimental data.

2. METHODOLOGY

2.1. Experimental setup and preparation of GNP-water nanofluids

The schematic view and figure of the designed and fabricated setup is presented in Figure 1. All components and procedure of the designed and fabricated test setup are explained in detail in supplementary information. Five necessary units are associated in this system such as cooling unit, heating part, flow loop, measuring devices and data analysis by connected PC through the software. However, the whole flow loop is connected with metallic pipes, a test section which is made of copper material, pump and a flow meter. The magnetic drive pump was used to allow the GNP-water nanofluids from 21 litter stainless jacketed tank to the flow loop at a flow rate of 0-20 litter/minute. Further, the pump flow was controlled by an inverter. The test section of copper material (length 1500 mm and inner diameter 4 mm) was used. The test section was wrapped by heating tape (maximum of 900 W) and covered with the hot insulation to avoid from heat loss. The K-type thermocouples were installed in the system to measure the surface, inlet, outlet and rest required temperatures. To measure the pressure drop, at inlet and outlet of

the test section a differential pressure transducer (DP) was installed. In this experiment we used the distilled water as the basefluid and graphene nanoparticles with surface area of 740 m^2/g were selected to prepare the nanofluid. The functionalized GNP-water nanofluids were used at concentrations of 0.025, 0.05, 0.075, and 0.1 wt%. A turbulent flow heat transfer range was considered the Reynolds range of 3900-11700. Two constant heat flux were considered at 18565 W/m^2 and 23870 W/m^2 respectively. To achieve the highly dispersed and stable GNP-water nanofluids, the covalent functionalization approach was used to prepare the sample. The detailed functionalization method and characterization approach is presented in our previous work [4].

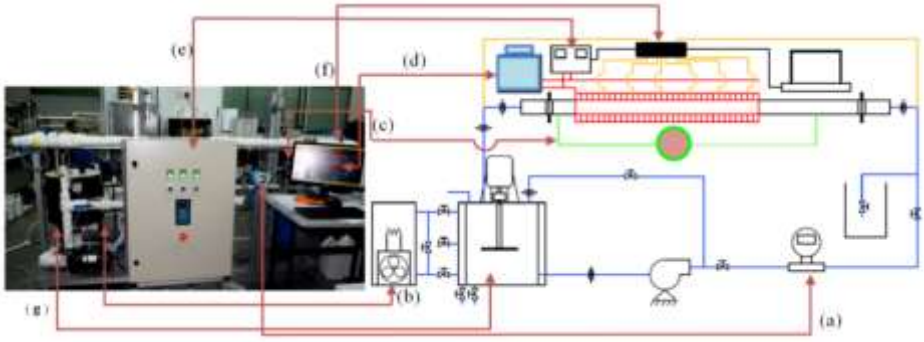

Figure 1. Experimental setup and lay out of the designed test rig [4].

2.2. Numerical investigation

The estimation of heat transfer plays a significant role because affects the operational conditions and the design. However, better the prediction, the higher the accuracy of heat transfer performance evaluation. We have chosen the two-phase model for this study, which defines that there are other mechanisms triggered by the relative motion between the nanoparticles and basefluid like thermal dispersion and thermophoresis.

2.2.1. Boundary conditions

Figure 2 presents the computational domain which is selected for numerical analysis GNP-water nanofluids. In this study, the fully developed turbulent inlet velocity flow was chosen. Further, the radius and length of the test section was 4 mm and 1500 mm, respectively. The uniform constant wall heat flux of 18565 W/m^2 and 23870 W/m^2 were applied at weight percentage ranging from 0.025 to 0.1 wt% in the basefluid and the Reynolds range from 3900 to 11700 was considered. However, a uniform axial velocity based on the temperature of $T_{in}=30^0C$ and Re are taken assumptions. Also, the no-sleep boundary condition has been considered on the wall for the basefluid are the nanoparticles. However, for this model, the nanoparticles are assumed as that of the basefluid at the inlet.

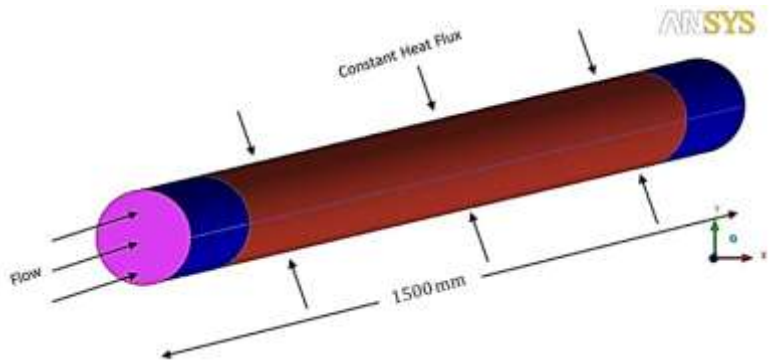

Figure 2. Computational domain of the test section.

2.2.2. Numerical method

In this study, ANSYS Fluent V15 was used to numerically measure and validate the heat transfer performance of nanofliuds. This model used the finite volume approach which can convert the governing partial differential equations into the discrete algebraic equations system [42]. However, in the discretization analysis normally second order upwind scheme are being selected for the turbulent kinetic energy, momentum and turbulent dissipation rate equations whereas upwind energy equation of first order is selected [43]. Therefore, for two phase intentions, the phase momentum equations with the shared pressure are resolved in coupled and segregated fashion. The two-phase mixture model based on a single fluid two phase approach, is used in the modeling by assuming that the coupling between two phases is sturdy and particles carefully trail the flow. Instead of utilizing the governing equation of each separately, the continuity, energy and momentum equations for the mixture are employed. Consequently, a nanofluid which was developed and composed of water and GNP flowing in a copper tube with even heating at the wall boundary is considered. Therefore, the dimensional equations for steady state mean conditions are given below:

a) Continuity equation

$$\nabla.(\rho_{eff}\,\overline{V}) = 0 \tag{1}$$

B) Momentum equation

$$\nabla.\left(\rho_{eff}\,\overline{V}\,\overline{V}\right) = -\nabla\overline{P} + \mu_{eff}\nabla^2\overline{V} - \rho_{eff}\nabla.(\overline{v'v'}) \tag{2}$$

C) Conservation of energy

$$\nabla.\left(\rho_{eff}C_{p,eff}\,\overline{V}\,\overline{T}\right) = -\nabla\left(\left(k_{eff} + k_t\right)\nabla\,\overline{T}\right) \tag{3}$$

Above, the symbols$\overline{T}$, $\overline{P}$ and $\overline{V}$ denotes the time averaged flow variables, and the symbol v' denotes the fluctuations in velocity. However, the factor in the momentum equation $\rho_{eff}\nabla.(\overline{v'v'})$ denotes the turbulent shear stress. The terms of k_{eff} and k_t denotes the turbulent thermal conductivity and effective molecular conductivity, correspondingly.

For the model flow in the turbulent regime, the standard $k-\varepsilon$ model could be employed, based on the Launder and Spalding study [44], who has considered the equations 4 – 7 as follows:

$$\nabla.(\rho_{eff}kV) = \nabla.[(\frac{\mu_t}{\sigma_k})\nabla(k)] + G_k - \rho_{eff}\varepsilon \tag{4}$$

$$\nabla.(\rho_{eff}\varepsilon V) = \nabla.[\frac{\mu_t}{\sigma_\varepsilon}\nabla\varepsilon] + \frac{\varepsilon}{k}(C_{1\varepsilon}G_k - C_{2\varepsilon}\rho_{eff}\varepsilon) \tag{5}$$

$$G_k = \mu_t\,(\nabla V + (\nabla V)^T, \mu_t = \rho_{eff}\,C_\mu\,\frac{k^2}{\varepsilon} \tag{6}$$

$$\sigma_\varepsilon = 1.30,\ \sigma_k = 1.00, C_\mu = 0.09\ \ C_{1\varepsilon} = 1.44, C_{2\varepsilon} = 1.92 \tag{7}$$

Where μ_t is the coefficient of viscosity in turbulent regime.

2.2.3. Mesh dependency

In this work, a horizontal turbulent flow heat generation metallic circular tube and an outer isothermal cylindrical boundary undergoing turbulent convection nanofluid flow have been focused. The meshing tool which was available in ANSYS has been used to construct to computational mesh. A horizontal tube with diameter of 4 mm and length of 1500 mm is simulated in this study. A two-dimensional geometry has been considered for the investigation. The flow direction, heat flux and constant temperature are illustrated in Figure 2. However, during the domain an organized mesh built on a rectangular grid was used. Though the radial lengths of the domain are separated into 40 mesh elements with a bias toward the top of the domain, the axial lengths are divided into 500 elements without any bias. The present model has around 20,000 elements. Figure 3 presents the assessment of Res versus Nus for basefluid as a working fluid at three diverse grid deliveries.

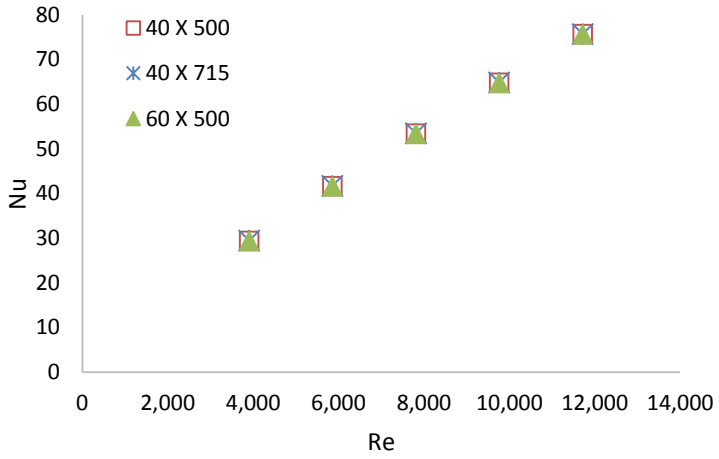

Figure 3. A comparison between Re and Nus for basefluid at three different grid distributions.

2.2.4. Simulation cases

The heat transfer characteristics of GNP-water nanofluid at 5 different Re numbers (3900, 5859, 7812, 9765 and 11700) and mass fractions of (0.025, 0.05, 0.075 and 0.1wt%) were investigated in a heated tube using two-phase mixture models. Considering 2 different constant wall heat fluxes of 18565 W/m^2 and 23870 W/m^2 on the tube wall, there are 50 simulation cases for this study.

3. RESULTS AND DISCUSSIONS

3.1. Functionalization analysis

Here we used the covalent functionalization approach to develop the propylene glycol-based graphene nanoplatelets based water (GNP-water) nanofluids. The functionalization method and the GNP-water nanofluids characterization results are explained in detail in our previous work [4]. Figure 5a presents the TEM and SEM images of the functionalized GNP. Further TEM image can show the flakes with fairly smooth surface and layer edge. However, from the SEM and TEM images it is difficult to identify the minute functional groups, but it could be observed the wrinkles and deterioration of the GNP that formed because of propylene glycol functionalization. From Figure 4 it could be observed that the structure of nanoparticles consists of stacked graphene layers.

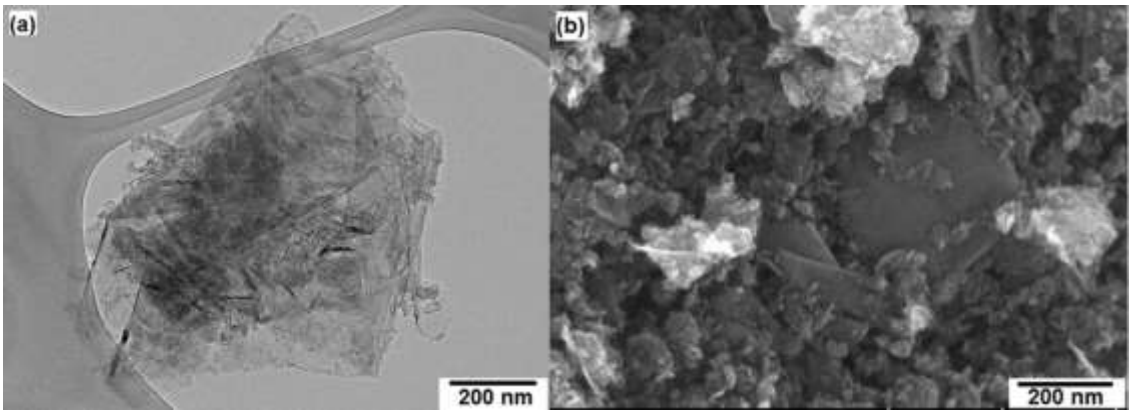

Figure 4. TEM (a) and SEM (b) images of functionalized GNP nanoparticles.

3.2. Thermo-physical properties

In thermophysical properties of nanofluids the viscosity is a significant property which governs the quality of heat transfer fluid. However, in commercial basefluids, the temperature is the core and effective parameter in viscosity of nanofluids. The Anton paar rheometer was used to measure the viscosity with maximum error of 2%. Before using the nanofluids it was calibrated with the distilled water. The viscosity value of distilled water is 1.034 that closely matches with its theoretical value at 20 ^{0}C. The relative deviation was obtained maximum up to 2.5%. in general, the viscosity of GNP-water nanofluids versus shear rate was investigated at the temperature range of 20^{0}C - 50^{0}C (see Figure 5). However, interestingly the higher concentration nanofluids which were up to 0.1 wt% showed the similar viscosity values compared to the lower concentration nanofluids which were 0.025 wt%. also, it could be observed from the figure that the viscosity value reduces in all concentrations with the rise in temperature and it decreased between 10% and 30%. It reveals that the loading of GNPs nanoparticles enhances the friction and flowing resistance of fluids which eventually reasons the upsurge of viscosity.

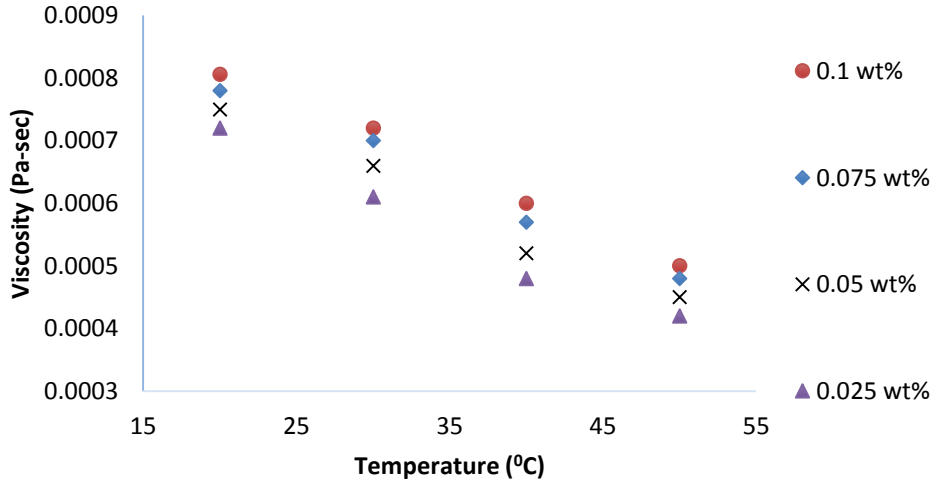

Figure 5. Viscosity of GNP-water nanofluids at different weight percentages.

Thermal conductivity is one of the significant parameters in the thermophysical properties of nanofluids. In this study thermal conductivity was measured by hot wire transient method (KD2 pro, decagon). The device was calibrated with the distilled water and the maximum error was found up to 2%. Table 1 presents the measured thermal conductivity values. The results reveal that it is a function of weight concentrations and temperature (see Table 2). However,

the enhancement in thermal conductivity with respect to the temperature could be attributed to the Brownian motion of the nanoparticles which are dispersed in the basefluid. Further, it was observed that as temperature increased so increase in thermal conductivity of nanofluids was obtained which simply could be the linear dependence of thermal conductivity increment on the temperature rise. All samples showed the good degree of enhancement in thermal conductivity. The maximum enhancement of thermal conductivity in GNP-water at 0.1wt% was measured up to 32% higher compared to the basefluid. Further, the density of GNP-water nanofluids have been investigated. More, to achieve the increase in pressure loss and friction factor the density of the nanoparticles is a significant parameter to measure. It was observed that density is a function of weight concentration and temperature (see Table 1). The density of the GNP-water nanofluids decreased by increasing the temperature, which reveals that the increment in volume of the liquid with increment in temperature. Also, there was rising trend between the density of GNP-water nanofluids and the weight percentage. Besides, the specific heat of GNP-water nanofluids was also measured. The effect of increased weight concentration and temperate on the heat capacity of GNP-water was analyzed. It was observed that the increase of weight concentration in GNP-water nanofluids produced a drop in the value of heat capacity, which was significant.

Table 1. Dynamic viscosity, specific heat, thermal conductivity and density of GNP-water nanofluids.

GNP-water nanofluids (concentration wt%)	Density (kg/ m^3)	Specific heat (J/kg-K)	Viscosity (Pa-s)	Thermal conductivity k, (W/m-K)
0.1	1055.863	2807.352	0.003129	0.85
0.075	1040.232	3058.304	0.002347	0.83
0.05	1025.058	3358.526	0.001705	0.81
0.025	1010.32	3724.108	0.001192	0.76

Table 2. Presents the thermal conductivity of GNP-water nanofluids at different weight concentrations and temperature.

Temperature (^{0}C)	DW (W/m-K)	0.1wt% (W/m-K)	0.075wt% (W/m-K)	0.05wt% (W/m-K)	0.025wt% (W/m-K)	Percentage Increase in 0.1wt% compared to DW
25	0.59	0.71	0.7	0.68	0.66	20.33
30	0.60	0.74	0.73	0.72	0.70	23.12
35	0.61	0.76	0.75	0.73	0.71	23.57
40	0.62	0.79	0.78	0.76	0.72	26.60
45	0.63	0.82	0.8	0.78	0.74	28.93
50	0.64	0.85	0.83	0.81	0.76	32.39

3.3. Numerical and experimental validation

The validation of the data is essential to authenticate the numerical results by comparing with the experimental and theoretical results. However, in this study the numerical results of basefulid (distilled water DW) at constant wall heat fluxes of 18565 W/m^2 and 23870 W/m^2 was compared with the experimental results along with the correlations of Gnielinski and Dittus-Boelter equations. The correlations are given in equation 8 and 9. Figure 6 presenting the experimental and numerical comparison for the tube surface temperature at different constant wall heat fluxes. However, it could be observed that the there is a linear growth in

surface temperature along the pipe and Re for both heat fluxes, representing a small amount of variation between experimental and numerical results (see Figure 6 a and b). Therefore, the results in Figure 6 clearly shows that there is a good agreement in the theoretical, numerical and experimental results. However, it was observed that when heat flux was increased from 18565 W/m^2 to 23870 W/m^2 then slight deviation in between numerical and experimental results also increased. The average deviation in between numerical results from experimental data was found up to 4% for the distilled water.

$$Nu = \frac{\left(\frac{f}{8}\right)(Re-1000)Pr}{1+12.7\left(\frac{f}{8}\right)^{0.5}\left(Pr^{\frac{2}{3}}-1\right)} \tag{8}$$

$$Nu = 0.0236\,[Re]^{0.8}\,[Pr]^{0.3} \tag{9}$$

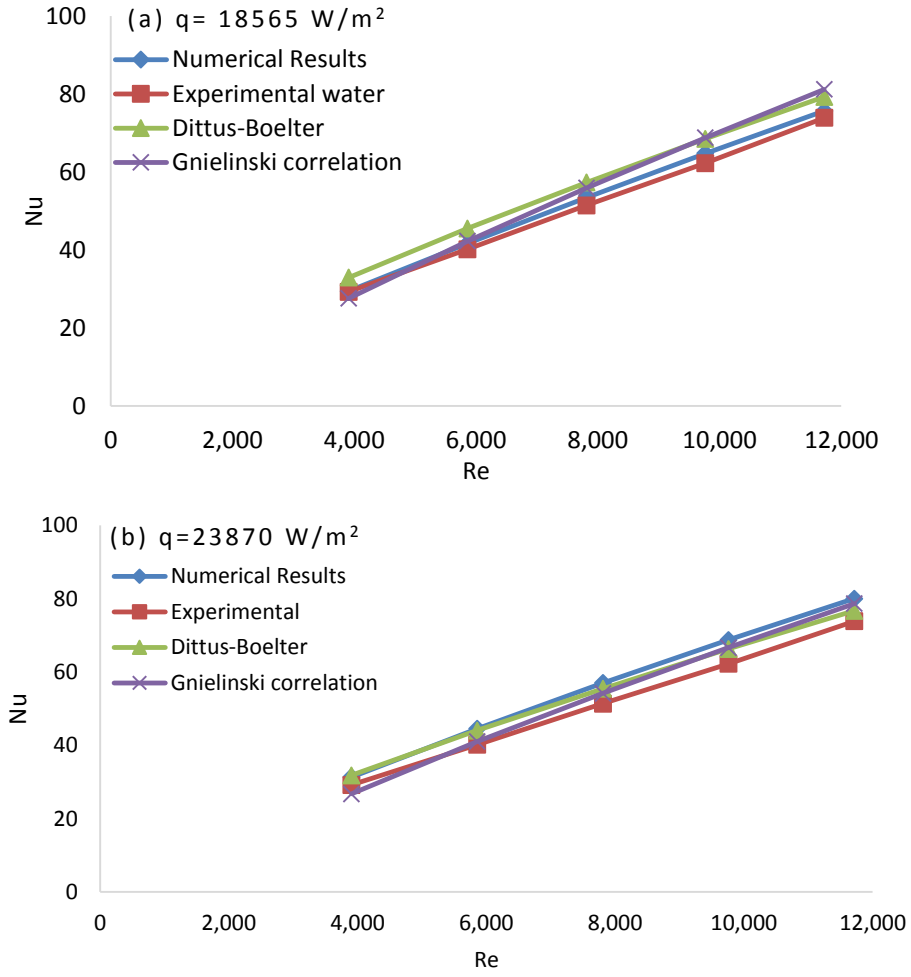

Figure 6. Comparison of Nus and various Res which were produced by two phase mixture method and also it compares the results with the correlations which were governed by Gnielinski and Dittus-Boelter.

3.4. Thermal analysis

For numerical study of GNP-water nanofluids, four concentrations were chosen (0.025, 0.05, 0.075 and 0.1 wt%) and 450 simulation cases were considered. The Re of 3900, 5859, 7812, 7965 and 11700 were considered. Figure 7 presents the heat transfer coefficient of GNP-water measured experimentally and numerically. The results show that by increasing the

concentration of GNP in basefluid it has a better heat transfer characteristic. Further it was observed that, by increasing the Re the deviation between the experimental and numerical wall temperature reduced and at higher Re value it had reverse effects. It could be detected that the heat transfer of GNP-water nanofluids is a function of the Re. It can be observed that some GNP-water sample lines with different slopes and they increase with the increase in the Re also along with the increase in the weight concentrations. However, it is a fact that the thermal performance of the basefluid is being improved by adding the amount of GNP nanoparticles.

Consequently, by adding nanoparticles, the performance of heat transfer depreciates because of dominant effect of viscosity associated with thermal properties. This spectacle could be credited to the enhanced thermal conductivity of GNP-water. However, about 119% increase in heat transfer coefficient of GNP-water was measured at the 0.1 wt% and at Re of 11700. This outcome was much more realized at the higher concertation of nanofluids by which the heat transfer rate was repressed. Though, it is understandable that the convective heat transfer is largely influenced by the lower molecular momentum diffusivity, nanoparticle size, flow rate, and increase in both thermal boundary layer thickness and viscosity.

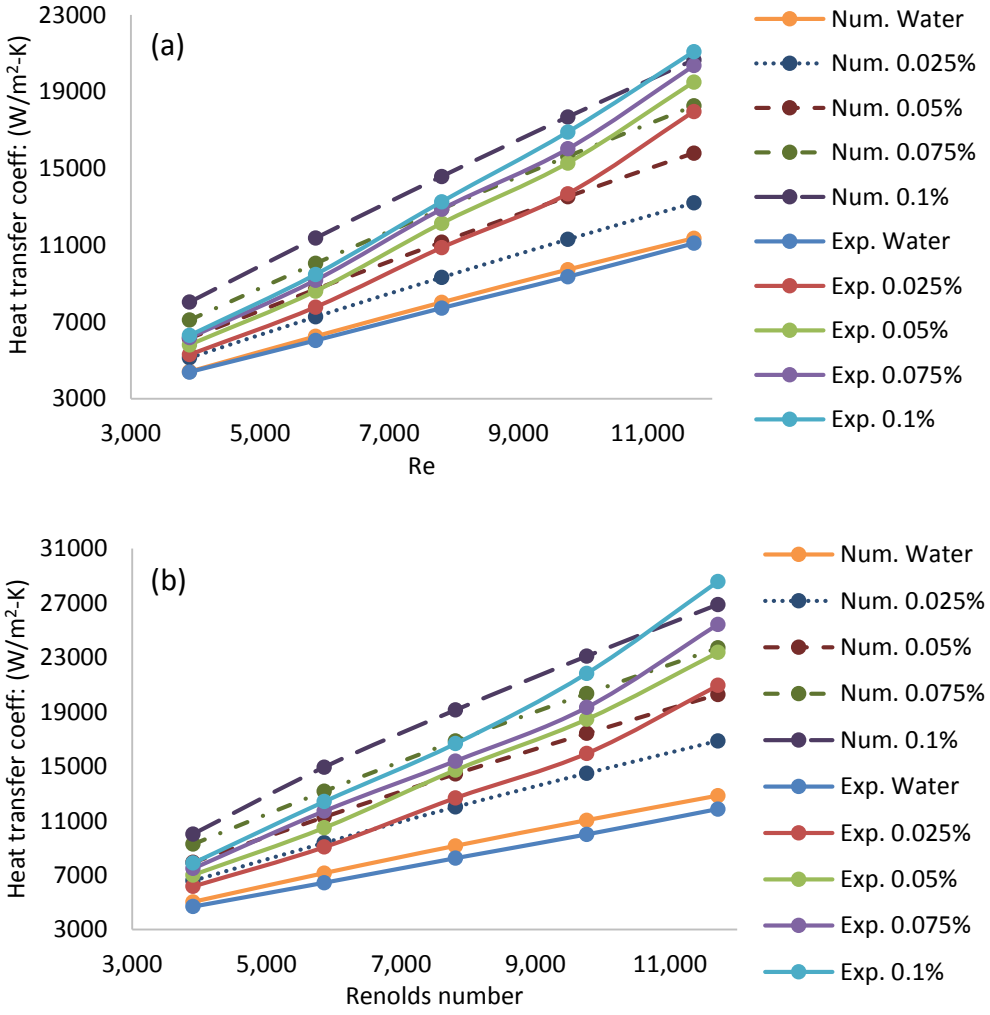

Figure 7. Experimental and numerical heat transfer performance of GNP-water at different heat fluxes and weight percentages.

In general, the numerical results show a slightly higher heat transfer coefficient then the experimental results. At both constant wall heat fluxes as shown in Figure 7 a and b, the maximum deviation of numerical simulation from the results of heat transfer coefficient is 3%.

However, all concentrations of GNP-water nanofluids were measured and compared with the numerical results which show the good agreement at both applied constant wall heat fluxes (see Figure 7).

Moreover, the Nu of GNP-water nanofluids was measured at two different heat fluxes and Re (see Figure 8). However, in both applied heat flux and all concentrations the Nu showed the good enhancement with increase in velocity for both experimental and numerical results. However, it could be seen that in Figure 8 that the average Nu augments with increase of Re. It is due to the fact that the velocity magnitude of the GNP-water nanofluid stream enhances as the Re increases. Besides, the kinetic energy upsurges which reasons that the Brownian effects becomes more actual. It could be seen in the figure 8 (a and b) some lines with different slopes, which increased the increase in the Re as well as concentration of GNP-water. In a curve fitting to the experimental data, the numerical results are closely fitting the experimental data. The consequence of weight concentration of GNP-water on Nu was observed as it significantly enhanced the Nu. It could be the reason of enhanced thermal conductivity and the abridged thermal resistance between the flowing fluid and the inner wall surface of the test section tube. The highest Nu of GNP-water at 23870 W/m^2 and 18565 W/m^2 and at 0.1 wt% in both numerical and experimental results was recorded up to 84% and 54%, respectively.

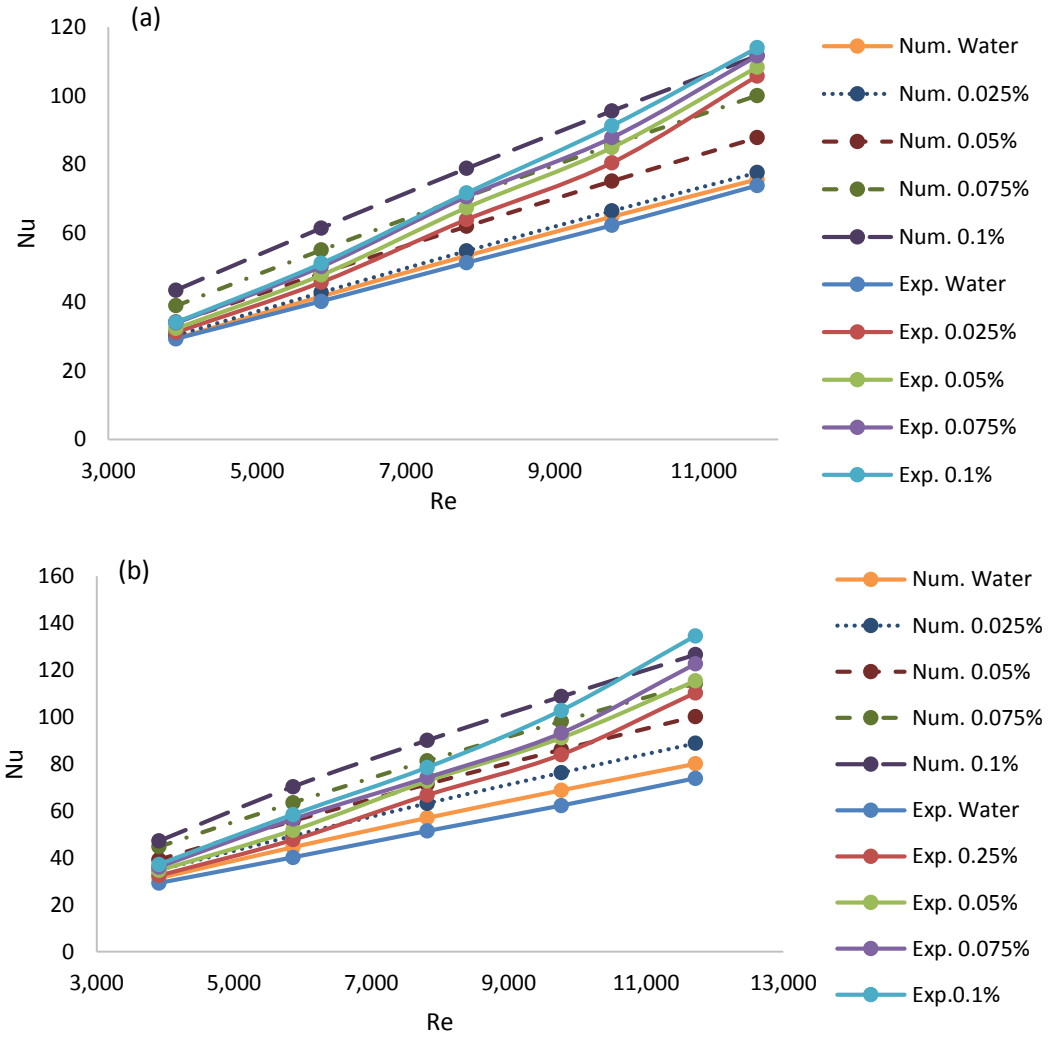

Figure 8. The Average Nu of GNP-water at different weight concentrations and Re at input power of (a) q= 18565 W/m^2 (b) q=23870 W/m^2.

3.5. Pressure drop

Before considering the nanofluids for practical applications, the fluid flow features of the nanoflids are very important to be explained in addition to the heat transfer performance measurements. The pressure drop study of nanofluids with basefluids delivers the suggestion about the pumping power necessities. It could be observed that if higher is the pressure loss then higher will be the Re for both the nanofluids and basefluid as presented in the Figure 9. However, the qualitative study of the Figure 9 exposes that the increasing trend of pressure loss is alike for all weight concentrations of GNP-water nanofluids. Therefore, it was found that the pressure drop increases with increasing in Re at different concentrations. The pressure drop also increases as the concentration of GNP-water nanofluids increases and the lowest value for pressure drop was obtained in the basefluid. Furthermore, the significant increase in the pressure drop was found with the increment in the concentration of GNP-water which is because of higher viscosity of GNP-water nanofluids (see Figure 9). The highest friction factor of the GNP-water nanofluids increased by 4 – 13.95% compared to the basefluid. However, it could be said that the higher viscosity of the nanofluids was due to the addition of GNP nanosheets in the basefluid which results in more pressure drop. Also, the increased pressure drop appear based on the viscous drag effects of the nanofluids. However, this expression can be evaluated from equation no 10, wherein the friction factor as a function of the pressure drop was mostly prejudiced by the density of the GNP nanofluids that caused from an increase in the GNP nanoparticle concentrations. It could be observed that this study confirms that the effect of GNP-water nanofluids addition on the viscosity of nanofluid and similarly on the pressure drop is important. Therefore, in the flow regime, the pressure drop is directly proportional to viscosity of fluid. This increment in viscosity leads to the undesired increase in pumping power. Consequently, the design structure of a heat exchanger for effective heat transfer and least pumping power is crucial in terms of energy savings and can reason considerable faults when assessing the performance of nanofluids (pumping power and heat transfer) in various thermal applications. Finally, the effect of two different constant wall heat fluxes on the pressure drop gradient at 0.1 wt% of GNP-water is presented in Figure 10.

$$f = \Delta P/((L/D)((\rho v\text{^}2)/2)) \tag{10}$$

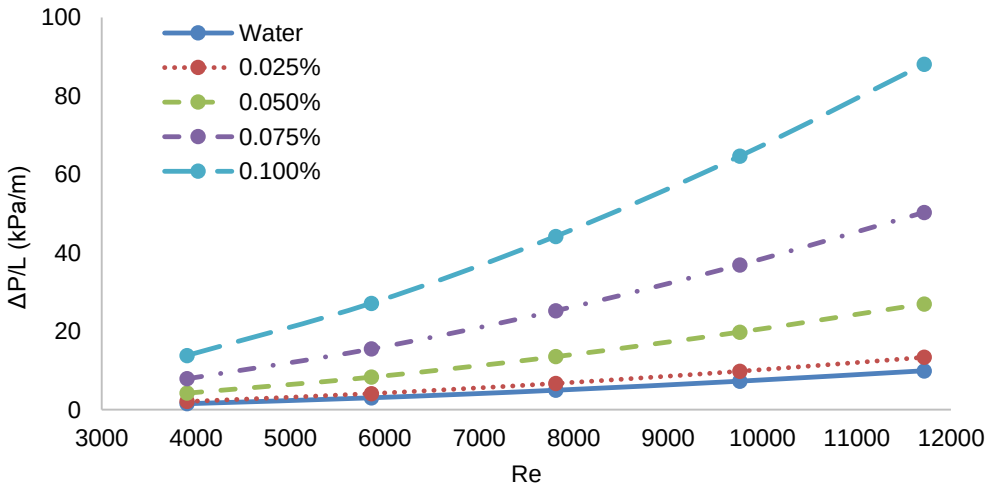

Figure 9. Pressure drop versus Re for GNP-water nanofluids with different weight concentrations as well as water.

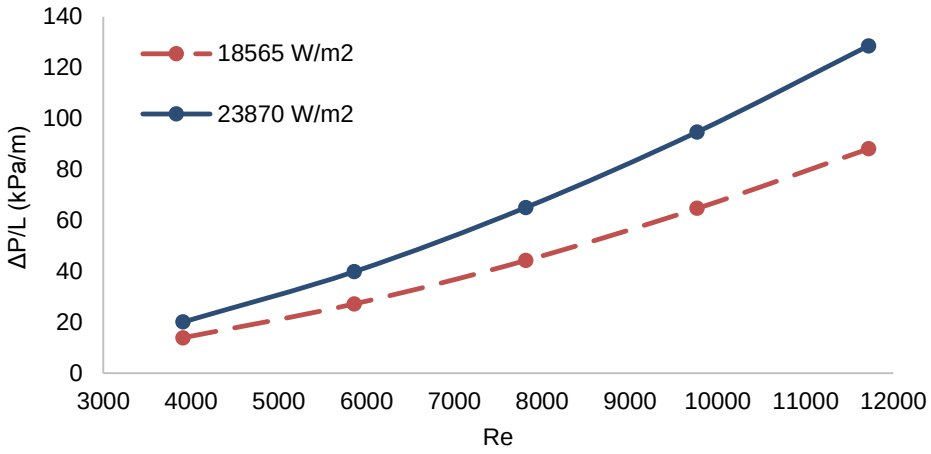

Figure 10. Pressure drop gradient for GNP-water nanofluids at 0.1% wt versus Re number at two different heat fluxes.

4. CONCLUSION

This study presented the numerical and experimental study of heat transfer and pressure loss characteristics of functionalized GNP-water nanofluids in a horizontal tube in a conduit flow. The covalently functionalized GNP-water nanofluids were used and the Reynold number range was considered from 3900-11700. Two constant wall heat fluxes of 18565 W/m^2 and 23870 W/m^2 was considered. For numerical analysis CFD two-phase mixture model was used. The validation results confirmed the applicability of Fluent to simulate heat transfer phenomena in the presence of GNP-water nanofluids. The main conclusions of this study are given below:

- The highly dispersed functionalized GNP-nanofluids significantly enhanced the heat transfer performance.
- The thermal conductivity of GNP-water at 0.1 wt% increased up to 32% which was dependent on temperature and concentration.
- The highest improvement in heat transfer coefficient of GNP-water nanofluids at heat flux of 23870 W/m2 and 0.1 wt% was achieved up to 119% and the highest friction factor increased in the range of 4 – 13.95%, respectively.
- A significant enhancement was achieved in thermal performance and the Nu by just adding the small amount of GNP nanoparticles. It was observed that the improved thermal conductivity and the reduced thermal resistance were offered by the functionalized GNP-water nanofluid in the inner surface of the copper test section.

ACKNOWLEDGEMENT

The authors wish to thank Universiti Teknologi Malaysia and Ministry of Higher Education, Malaysia for their cooperation and assistance throughout conducting this research. Special appreciation to the Research Management Centre of UTM for the financial support through the RUG funding QJ130000.2409.04G39 and QJ130000.2509.16H21.

NOMENCLATURE

Nomenclature	Greek symbols	Subscripts
D Diameter, m	ΔP Pressure drop (Pa)	w Tube wall
L Tube length, m	ή Efficiency of loop	p Particles
Cp Specific heat ($Jkg^{-1}K^{-1}$)	Ɛ Performance index	nf Nanofluid
Pe Peclet number	μ Viscosity (Pa-s)	bf Basefluid
V velocity (ms^{-1})	ρ Density ($Kg\ m^{-3}$)	ID Inner diameter
n Number of Tubes		b Bulkfluid
q Heat transfer (W)		out outlet
Nu Nu		OD Outer diameter
m^o Mass flow rate kg/s		Tb Bulk temperature
Re Re		in inlet
U Velocity, m/s		
T Temperature, °C		
W pumping power		
k Thermal conductivity ($W\ m^{-1}K^{-1}$)		
H Heat transfer coefficient ($W\ m^{-2}\ K^{-1}$)		
Pr Prandtl number		
A Area (m^2)		
F Friction factor		

REFERENCES

[1] Naphon, P., Wiriyasart, S., Arisariyawong, T., and Nakharintr, L., ANN, numerical and experimental analysis on the jet impingement nanofluids flow and heat transfer characteristics in the micro-channel heat sink. International Journal of Heat and Mass Transfer, 2019. 131: p. 329-340.

[2] Qi, C., Liu, M., Wang, G., Pan, Y., and Liang, L., Experimental research on stabilities, thermophysical properties and heat transfer enhancement of nanofluids in heat exchanger systems. Chinese Journal of Chemical Engineering, 2018. 26(12): p. 2420-2430.

[3] Setareh, M., Saffar-Avval, M., and Abdullah, A., Experimental and numerical study on heat transfer enhancement using ultrasonic vibration in a double-pipe heat exchanger. Applied Thermal Engineering, 2019. 159: p. 113867.

[4] Solangi, K.H., Amiri, A., Luhur, M.R., Ghavimi, S.A.A., Zubir, M.N.M., Kazi, S.N., and Badarudin, A., Experimental investigation of the propylene glycol-treated graphene nanoplatelets for the enhancement of closed conduit turbulent convective heat transfer. International Communications in Heat and Mass Transfer, 2016. 73: p. 43-53.

[5] Teng, K.H., Kazi, S.N., Amiri, A., Habali, A.F., Bakar, M.A., Chew, B.T., Al-Shamma'a, A., Shaw, A., Solangi, K.H., and Khan, G., Calcium carbonate fouling on double-pipe heat exchanger with different heat exchanging surfaces. Powder Technology, 2017. 315: p. 216-226.

[6] Aman, S., Khan, I., Ismail, Z., Salleh, M.Z., and Tlili, I., A new Caputo time fractional model for heat transfer enhancement of water based graphene nanofluid: An application to solar energy. Results in Physics, 2018. 9: p. 1352-1362.

[7] Bahiraei, M., Kiani Salmi, H., and Safaei, M.R., Effect of employing a new biological nanofluid containing functionalized graphene nanoplatelets on thermal and hydraulic

characteristics of a spiral heat exchanger. Energy Conversion and Management, 2019. 180: p. 72-82.

[8] Ghasemi, S.E., Ranjbar, A.A., and Hosseini, M.J., Forced convective heat transfer of nanofluid as a coolant flowing through a heat sink: Experimental and numerical study. Journal of Molecular Liquids, 2017. 248: p. 264-270.

[9] Bai, Y., Wang, L., Zhang, S., Lin, X., and Chen, H., Numerical analysis of a closed loop two-phase thermosyphon under states of single-phase, two-phase and supercritical. International Journal of Heat and Mass Transfer, 2019. 135: p. 354-367.

[10] Burk, B.E., Grumstrup, T.P., Bevis, T.A., Kotovsky, J., and Bandhauer, T.M., Computational examination of two-phase microchannel heat transfer correlations with conjugate heat spreading. International Journal of Heat and Mass Transfer, 2019. 132: p. 68-79.

[11] Ogawa, S. and Usui, S., Heat Transfer Enhancement by Vortex Generators for Compact Heat Exchanger of Automobiles. Open Journal of Fluid Dynamics, 2018. 8: p. 321-330.

[12] Sajjad, M., Kamran, M.S., Shaukat, R., and Zeinelabdeen, M.I.M., Numerical investigation of laminar convective heat transfer of graphene oxide/ethylene glycol-water nanofluids in a horizontal tube. Engineering Science and Technology, an International Journal, 2018. 21(4): p. 727-735.

[13] Cárdenas Contreras, E.M., Oliveira, G.A., and Bandarra Filho, E.P., Experimental analysis of the thermohydraulic performance of graphene and silver nanofluids in automotive cooling systems. International Journal of Heat and Mass Transfer, 2019. 132: p. 375-387.

[14] Das, S., Giri, A., Samanta, S., and Kanagaraj, S., Role of graphene nanofluids on heat transfer enhancement in thermosyphon. Journal of Science: Advanced Materials and Devices, 2019. 4(1): p. 163-169.

[15] Ghozatloo, A., Rashidi, A., and Shariaty-Niassar, M., Convective heat transfer enhancement of graphene nanofluids in shell and tube heat exchanger. Experimental Thermal and Fluid Science, 2014. 53: p. 136-141.

[16] Huminic, G. and Huminic, A., Hybrid nanofluids for heat transfer applications – A state-of-the-art review. International Journal of Heat and Mass Transfer, 2018. 125: p. 82-103.

[17] Javanmard, M., Taheri, M.H., Abbasi, M., and Ebrahimi, S.M., Heat transfer analysis of hydromagnetic water–graphene oxide nanofluid flow in the channel with asymmetric forced convection on walls. Chemical Engineering Research and Design, 2018. 136: p. 816-824.

[18] Mehrali, M., Sadeghinezhad, E., Akhiani, A.R., Tahan Latibari, S., Talebian, S., Dolatshahi-Pirouz, A., Metselaar, H.S.C., and Mehrali, M., An ecofriendly graphene-based nanofluid for heat transfer applications. Journal of Cleaner Production, 2016. 137: p. 555-566.

[19] Nazari, M.A., Ghasempour, R., Ahmadi, M.H., Heydarian, G., and Shafii, M.B., Experimental investigation of graphene oxide nanofluid on heat transfer enhancement of pulsating heat pipe. International Communications in Heat and Mass Transfer, 2018. 91: p. 90-94.

[20] Ranjbarzadeh, R., Karimipour, A., Afrand, M., Isfahani, A.H.M., and Shirneshan, A., Empirical analysis of heat transfer and friction factor of water/graphene oxide nanofluid flow in turbulent regime through an isothermal pipe. Applied Thermal Engineering, 2017. 126: p. 538-547.

[21] Baby, T.T. and Sundara, R., A facile synthesis and field emission property investigation of Co3O4 nanoparticles decorated graphene. Materials Chemistry and Physics, 2012. 135(2): p. 623-627.

[22] Zhou, Y., Cui, X., Weng, J., Shi, S., Han, H., and Chen, C., Experimental investigation of the heat transfer performance of an oscillating heat pipe with graphene nanofluids. Powder Technology, 2018. 332: p. 371-380.

[23] Hussien, A.A., Abdullah, M.Z., Yusop, N.M., Al-Nimr, M.d.A., Atieh, M.A., and Mehrali, M., Experiment on forced convective heat transfer enhancement using MWCNTs/GNPs hybrid nanofluid and mini-tube. International Journal of Heat and Mass Transfer, 2017. 115: p. 1121-1131.

[24] Naddaf, A., Zeinali Heris, S., and Pouladi, B., An experimental study on heat transfer performance and pressure drop of nanofluids using graphene and multi-walled carbon nanotubes based on diesel oil. Powder Technology, 2019. 352: p. 369-380.

[25] Vallejo, J.P., Żyła, G., Fernández-Seara, J., and Lugo, L., Rheological behaviour of functionalized graphene nanoplatelet nanofluids based on water and propylene glycol:water mixtures. International Communications in Heat and Mass Transfer, 2018. 99: p. 43-53.

[26] Yarmand, H., Zulkifli, N.W.B.M., Gharehkhani, S., Shirazi, S.F.S., Alrashed, A.A.A.A., Ali, M.A.B., Dahari, M., and Kazi, S.N., Convective heat transfer enhancement with graphene nanoplatelet/platinum hybrid nanofluid. International Communications in Heat and Mass Transfer, 2017. 88: p. 120-125.

[27] Sadeghinezhad, E., Togun, H., Mehrali, M., Sadeghi Nejad, P., Tahan Latibari, S., Abdulrazzaq, T., Kazi, S.N., and Metselaar, H.S.C., An experimental and numerical investigation of heat transfer enhancement for graphene nanoplatelets nanofluids in turbulent flow conditions. International Journal of Heat and Mass Transfer, 2015. 81: p. 41-

[28] El-Bouri, W., Deiab, I., Khanafer, K., and Wahba, E., Numerical and experimental analysis of turbulent flow and heat transfer of minimum quantity lubrication in a turning process using discrete phase model. International Communications in Heat and Mass Transfer, 2019. 104: p. 23-32.

[29] Kumar, V. and Sarkar, J., Two-phase numerical simulation of hybrid nanofluid heat transfer in minichannel heat sink and experimental validation. International Communications in Heat and Mass Transfer, 2018. 91: p. 239-247.

[30] Lee, J., O'Neill, L.E., Lee, S., and Mudawar, I., Experimental and computational investigation on two-phase flow and heat transfer of highly subcooled flow boiling in vertical upflow. International Journal of Heat and Mass Transfer, 2019. 136: p. 1199-1216.

[31] Liang, G. and Mudawar, I., Review of single-phase and two-phase nanofluid heat transfer in macro-channels and micro-channels. International Journal of Heat and Mass Transfer, 2019. 136: p. 324-354.

[32] Naemsai, T., Kammuang-lue, N., Terdtoon, P., and Sakulchangsatjatai, P., Numerical model of heat transfer characteristics for sintered-grooved wick heat pipes under non-uniform heat loads. Applied Thermal Engineering, 2019. 148: p. 886-896.

[33] Peng, D., Lu, Y., Zhang, C., Yu, Q., and Wu, Y., Numerical study of heat transfer characteristic on the melting process of quaternary mixed nitrate. Applied Thermal Engineering, 2019. 158: p. 113766.

[34] Setareh, M., Saffar-Avval, M., and Abdullah, A., Experimental and Numerical Study on Heat Transfer Enhancement Using Ultrasonic Vibration in a Double-Pipe Heat Exchanger. Applied Thermal Engineering, 2019: p. 113867.

[35] Wang, M., Liu, L., Zhang, X.-Y., Chen, L., Wang, S.-Q., and Jia, Y.-H., Experimental and numerical investigations of heat transfer and phase change characteristics of cemented paste backfill with PCM. Applied Thermal Engineering, 2019. 150: p. 121-131.

[36] Yu, S., Chen, J., Mi, X., Lu, L., Ding, G., and Ding, C., Experimental and numerical investigation of two-phase flow outside tube bundle of liquefied natural gas spiral wound heat exchangers under offshore conditions. Applied Thermal Engineering, 2019. 152: p. 103-112.

[37] Shah, S. and Kumar, K., Experimental Study & Heat Transfer Analysis on Copper Spiral Heat Exchanger Using Water Based SiO2 Nanofluid as Coolant. . World Journal of Nano Science and Engineering, 2018. 8: p. 57-68.

[38] Moosavian, S.M., Rahim, N.A., Selvaraj, J., and Solangi, K.H., Energy policy to promote photovoltaic generation. Renewable and Sustainable Energy Reviews, 2013. 25: p. 44-58.

[39] Sadri, R., Hosseini, M., Kazi, S.N., Bagheri, S., Zubir, N., Solangi, K.H., Zaharinie, T., and Badarudin, A., A bio-based, facile approach for the preparation of covalently functionalized carbon nanotubes aqueous suspensions and their potential as heat transfer fluids. Journal of Colloid and Interface Science, 2017. 504: p. 115-123.

[40] Solangi, K.H., Islam, M.R., Saidur, R., Rahim, N.A., and Fayaz, H., A review on global solar energy policy. Renewable and Sustainable Energy Reviews, 2011. 15(4): p. 2149-2163.

[41] Liu, C., Fang, H., Qiao, Y., Zhao, J., and Rao, Z., Properties and heat transfer mechanistic study of glycerol/choline chloride deep eutectic solvents based nanofluids. International Journal of Heat and Mass Transfer, 2019. 138: p. 690-698.

[42] Arzani, H.K., Amiri, A., Kazi, S.N., Chew, B.T., and Badarudin, A., Experimental and numerical investigation of thermophysical properties, heat transfer and pressure drop of covalent and noncovalent functionalized graphene nanoplatelet-based water nanofluids in an annular heat exchanger. International Communications in Heat and Mass Transfer, 2015. 68: p. 267-275.

[43] Behroyan, I., Ganesan, P., He, S., and Sivasankaran, S., Turbulent forced convection of Cu–water nanofluid: CFD model comparison. International Communications in Heat and Mass Transfer, 2015. 67: p. 163-172.

[44] Launder, B.E. and Spalding, D., The numerical computation of turbulent flows. Computer methods in applied mechanics and engineering, 1974. 3(2): p. 269-289.